ACS Catalysis

pubs.acs.org/acscatalysis Research Article

Controlling Non-Native Cobalamin Reactivity and Catalysis in the Transcription Factor CarH

Xinhang Yang, Benjamin H. R. Gerroll, Yuhua Jiang, Amardeep Kumar, Yasmine S. Zubi, Lane A. Baker, and Jared C. Lewis*

Cite This: *ACS Catal.* 2022, 12, 935−942 Read Online

ACCESS | Metrics & More | Article Recommendations | Supporting Information

ABSTRACT: Vitamin B_{12} derivatives catalyze a wide range of organic transformations, but B_{12}-dependent enzymes are underutilized in biocatalysis relative to other metalloenzymes. In this study, we engineered a variant of the transcription factor CarH, called CarH*, that catalyzes styrene C−H alkylation with improved yields (2−6.5-fold) and selectivity relative to cobalamin. While the native function of CarH involves transcription regulation via adenosylcobalamin (AdoCbl) Co(III)−carbon bond cleavage and *β*-hydride elimination to generate 4′,5′-didehydroadenosine, CarH*-catalyzed styrene alkylation proceeds via non-native oxidative addition and olefin addition coupled with a native-like *β*-hydride elimination. Mechanistic studies on this reaction echo findings from earlier studies on AdoCbl homolysis to suggest that CarH* selectivity results from its ability to impart a cage effect on radical intermediates. These findings lay the groundwork for the development of B_{12}-dependent enzymes as catalysts for non-native transformations.

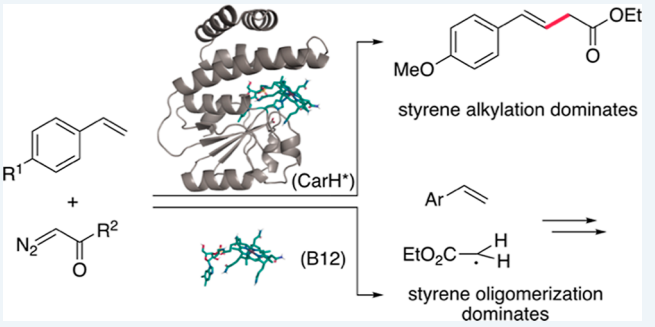

KEYWORDS: *B_{12}, cobalamin, C−H functionalization, biocatalysis, non-native enzyme catalysis*

INTRODUCTION

Derivatives of vitamin B_{12} comprise a family of cobalt corrin complexes (cobalamins) with different axial ligands that confer unique reactivity to these complexes in their roles as enzyme cofactors (Figure 1A).[1] B_{12}-dependent enzymes include adenosylcobalamin (AdoCbl)-dependent isomerases,[2] methylcobalamin (MeCbl)-dependent methyltransferases,[3] and dehalogenases.[4] Within these classes, variation of the axial ligand distal to the substrate binding pocket is also observed. The dimethylbenzimidazole (dmb) ligand of cobalamins can be bound to the cobalt center (dmb-on), as in class II B_{12}-dependent isomerases, or unbound (dmb-off), as in class I B_{12}-dependent isomerases.[2] In the latter case, a distal histidine residue from the protein scaffold can bind the cobalt center in a dmb-off/His-on fashion.[5] These structural variations and the unique interactions between cobalamins and their respective enzyme scaffolds enable these naturally occurring organometallic complexes to engage substrates via both radical and polar chemistry.[6]

When removed from their natural protein scaffolds, cobalamins can catalyze an even broader range of C−C bond-forming reactions than those observed in nature.[7] Moreover, Co(III)−alkyl complexes analogous to AdoCbl and MeCbl have been proposed as intermediates in reductive dehalogenation,[8] alkyl halide and alkene coupling reactions,[9] and a number of transformations involving alkenyl C−H functionalization.[10−12] These reactions proceed via a highly nucleophilic Co(I) intermediate[13] that undergoes oxidative addition with a variety of organic electrophiles to generate Co(III)−alkyl complexes.[14] These complexes can react via radical coupling or olefin addition pathways to generate different organic products. Unlike enzymatic transformations, however, product mixtures are typically obtained due to homolysis of the Co(III)−alkyl bond and subsequent free radical chemistry, and very few of these reactions can be achieved with catalyst-controlled selectivity.[7] We were therefore drawn to the potential non-native reactivity of cobalamin-containing proteins and the control that protein scaffolds could exert over the reactivity of cobalamin−alkyl intermediates.

Homolysis of the Co(III)−carbon bond of the AdoCbl cofactor in B_{12}-dependent isomerases (Figure 1B) forms the basis of a variety of C−H functionalization reactions that proceed via C−H abstraction by the 5′-deoxyadenosyl radical (Ado$^{\bullet}$).[2] We reasoned that similar active-site localization of a Co(III)−alkyl complex generated from the reaction of the

Received: October 14, 2021
Revised: December 13, 2021
Published: December 30, 2021

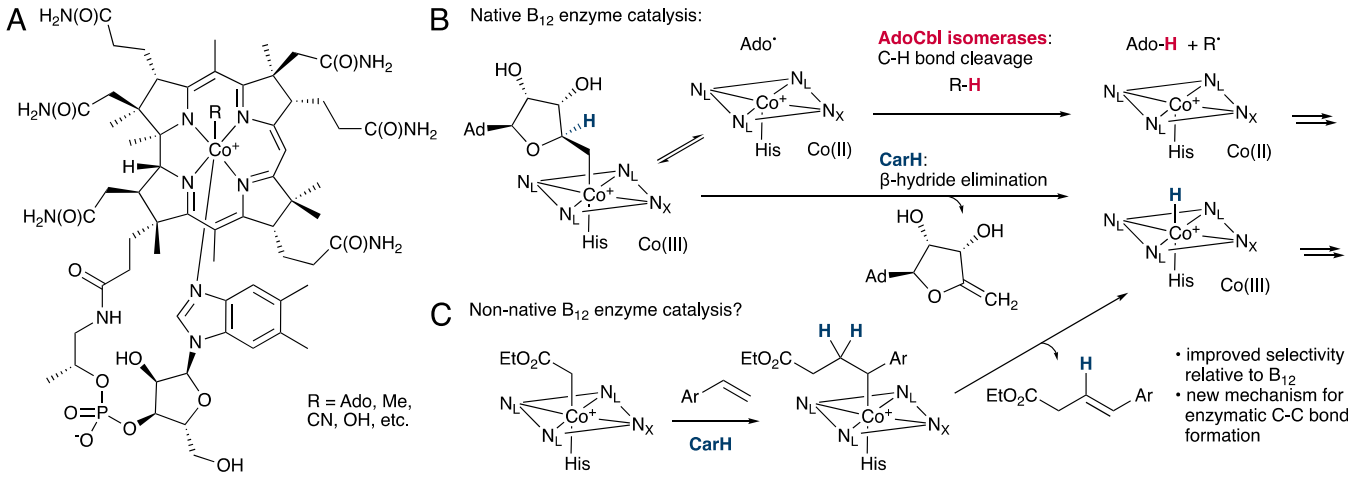

Figure 1. (A) Structures of representative cobalamins. (B) Comparison of the intermolecular C−H abstraction observed for AdoCbl-dependent isomerases[2] and a proposed radical-based β-hydride elimination mechanism for CarH (Ad = adenine).[16] (C) Potential CarH-catalyzed styrene C−H functionalization involving β-hydride elimination.

Co(I) form [cob(I)alamin] of a suitable cobalamin-containing protein with simple organic electrophiles could be used to confer selectivity to a variety of cobalt-catalyzed transformations. The light-dependent transcription factor CarH[15] piqued our interest as a candidate enzyme due to its proposed mechanism involving β-hydride elimination of an AdoCbl intermediate (Figure 1B).[16] If an analogous intermediate could be accessed via initial alkylation of Co(I) with a simple alkyl electrophile lacking β-hydrogen substituents,[14] reaction of the resulting Co(III)−alkyl with a reagent capable of generating an intermediate with β-hydride substituents could enable olefin formation[17] and catalyst turnover.

In considering reactions that could test this hypothesis, we were drawn to a study by Gryko involving β-alkylation of styrenes using alkyl diazoacetates catalyzed by the hexamethyl ester of CNCbl.[10] This reaction was proposed to proceed via radical addition of a Co(III)−carboxymethyl species to styrene, followed by β-hydride elimination (Figure 1C), the latter mirroring a proposed radical pathway for native CarH reactivity[16] (a polar mechanism was also proposed).[16,18] An undesired alkane byproduct also forms under the reaction conditions (~2:1) and was proposed to result from free-radical side reactions. Herein, we show that an engineered variant of CarH corrects this issue and increases styrene alkylation yields relative to cobalamin by stabilizing Co(III)−alkyl species generated from different organic electrophiles to enable selective reaction of these species with styrenes. This non-native reactivity suggests that cobalamin-containing proteins could serve as catalysts for a wide range of Co-catalyzed transformations.

RESULTS

CarH is a B_{12}-dependent transcription factor that exploits a remarkable exaptation of AdoCbl Co(III)−carbon bond cleavage[18,19] to enable light-activated gene expression,[15] rather than the more common radical rearrangement processes catalyzed by AdoCbl-dependent enzymes (Figure 1B).[2] In its AdoCbl-bound form, CarH forms a tetramer that binds DNA to repress transcription of carotenoid biosynthesis genes that protect organisms from light damage.[20] Upon exposure to light, the Co(III)−carbon bond of AdoCbl most likely undergoes homolytic cleavage[19] (although heterolytic cleavage has also been proposed[18]), leading to loss of 4′,5′-anhydroadenosine[16] and formation of bis-His cobalamin,[18] which causes a conformational change in the enzyme that favors monomer formation, DNA dissociation, and transcription activation. The structure of CarH comprises a C-terminal domain that binds AdoCbl in a dmb-off/His-on fashion (H177), a four-helix cap above the AdoCbl cofactor, and a N-terminal DNA-binding domain.[20]

We reasoned that apo-CarH could be reconstituted with hydroxocobalamin[18] which would be protonated to give aquocobalamin at pH 7.5[21] so that the vacant Ado-binding site could be used for substrate binding and that dmb-off/His-on cobalamin binding could allow for modulation of reactivity via distal axial ligand variation. We first examined CarH from *Thermus thermophilus* (*Tt*CarH), but its low solubility complicated characterization. This issue was addressed by fusing a N-terminal His_6-MBP tag to the enzyme, which we also presumed would disrupt potential tetramer formation. A histidine residue (H132) near the Ado binding pocket was mutated to glycine to preclude its binding to the Co center of cobalamin[18] and potential reactions with added electrophiles. Apo MBP-*Tt*CarH H132G (hereafter CarH*) was expressed in *Escherichia coli* (20 mg/L), purified by Ni-NTA chromatography, and reconstituted with a threefold excess of hydroxocobalamin. The enzyme was purified by size-exclusion chromatography to provide the desired cobalamin-bound form of CarH* as a monomer in good yield (84%).

The feasibility of reducing CarH* to its cob(I)alamin form and alkylating this species with different electrophiles was next evaluated. Several chemical reductants can be used to generate cob(I)alamin,[14] but most of these are heterogeneous or absorb UV−vis light at wavelengths that overlap with diagnostic absorptions for the different oxidation states of cobalamin. We therefore turned to UV−vis absorption spectroelectrochemistry to generate the cob(I)alamin form of CarH* and monitor its reaction with ethyl diazoacetate (EDA, Figure 2A), ethyl chloroacetate (ECA), and *p*-methoxystyrene. At a potential of −1.5 V, reduction of CarH* occurred, as evidenced by the appearance of a peak at 388 nm, consistent with cob(I)alamin (**ii**), and concomitant loss of a peak at 357 nm, associated with aquocob(III)alamin (**i**) (Figure 2B).[22] Addition of either EDA or ECA to **ii** led to rapid (<15 s) formation of cob(II)alamin

https://doi.org/10.1021/acscatal.1c04748
ACS Catal. 2022, 12, 935−942

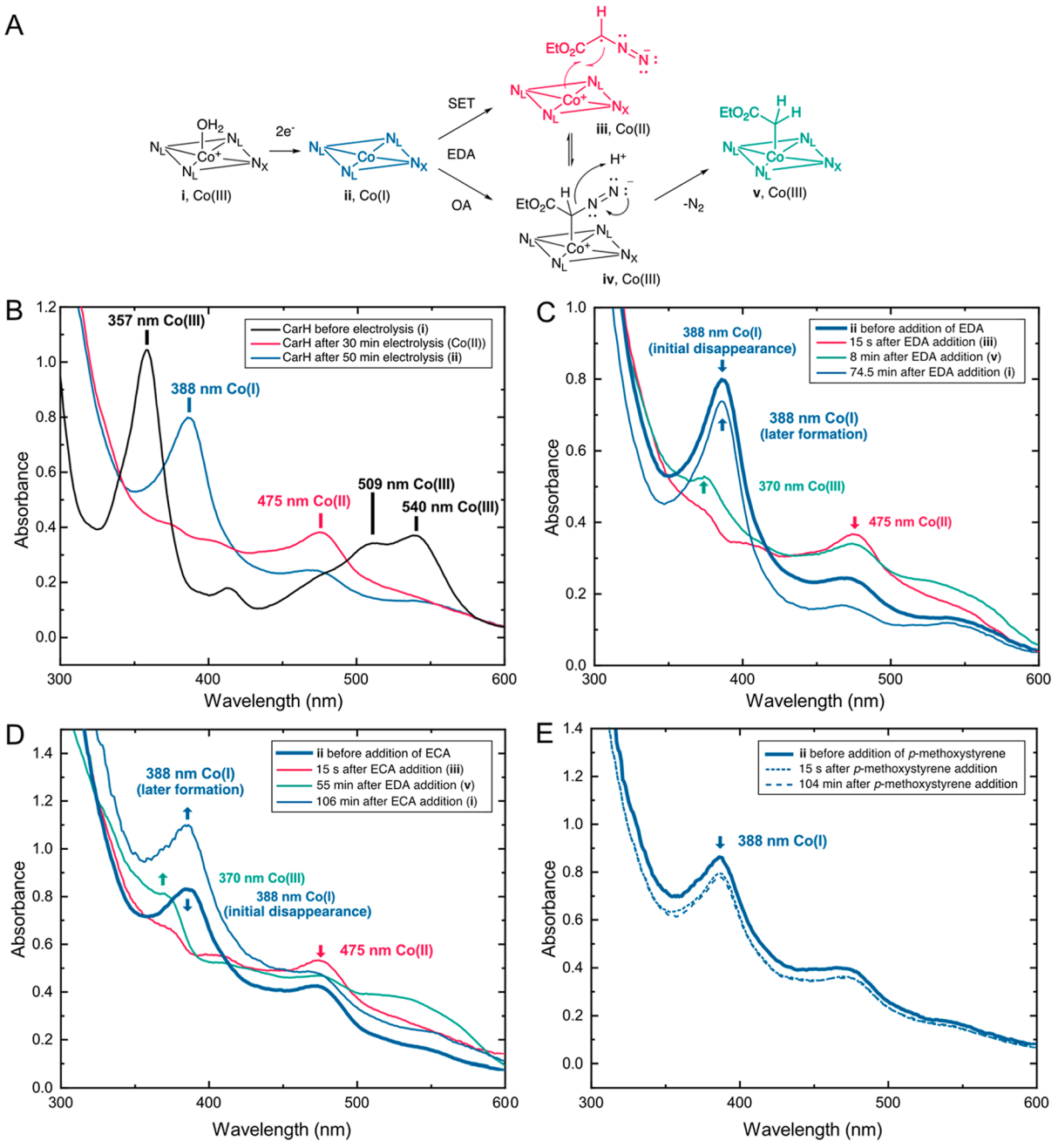

Figure 2. (A) Scheme for electrochemical reduction and reaction of CarH* with EDA. (B) UV−vis absorbance spectra for the cob(III)-, cob(II)-, and cob(I)alamin forms of CarH* (22 μM) generated following electrolysis for the specified times. Arrows indicate direction of absorbance change for different species. (C−E) UV−vis absorbance spectra for CarH* (22 μM) following addition of 22 μM EDA (C), ECA (D), or styrene (E).

(**iii**), as indicated by a peak at 475 nm (Figure 2C,D). A gradual disappearance of cob(II)alamin and appearance of a second cob(III)alamin species, assigned as **v** (presumably via the intermediacy of **iv**),[22] then occurred before reduction of the sample back to cob(I)alamin. The absorbances associated with **v** were red-shifted by roughly 18 nm and broadened relative to those associated with **i**, consistent with previously reported spectra of cobalamin complexes with increasingly less electronegative axial ligands[23] (from oxygen to carbon in the current case). It should also be noted that cob(II)alamin could also be formed from reduction of protons in water by **ii**,[24] and **v** could form via two-electron oxidative addition of **ii**, so the relevance of the observed cob(II)alamin peaks to the formation of **v** cannot be definitively established from these data. No significant buildup of peaks consistent with cob(III)alamin was observed upon addition of styrene (Figure 2E). Similar spectra were observed for the reaction of ECA with cob(I)alamin at −1.2 V, but the rates of the reactions were much faster, presumably due to improved access of cobalamin to the electrode in the absence of the CarH* protein components (Supporting Information Figure S1C). Interestingly, a peak corresponding to a Co(III) species following addition of EDA to cob(I)alamin was not red-shifted as it was for CarH*, suggesting that intermediate **v** does not build up for cobalamin in solution as it does within CarH* (Supporting Information Figure S1B).

Encouraged by the observation of a cob(III)alamin species consistent with ethyl carboxymethyl intermediate **v** envisioned

https://doi.org/10.1021/acscatal.1c04748
ACS Catal. 2022, 12, 935−942

in Figure 1, we next sought to establish whether subsequent reaction of this species would occur in the presence of styrene. Toward this end, *p*-methoxystyrene and EDA were incubated with 4.4 mol % of CarH* and excess Ti(III) citrate, which have been used to access Co(I) in a variety of Co-catalyzed transformations.[7] Alkene **1a** formed in 57% yield, constituting 13 turnovers under optimized reaction conditions (Table 1, entry 1). A small amount of alkane **2a** also formed (**1a**:**2a** = 19:1). A significantly lower yield of **1a** (22%) and lower selectivity for **1a** over **2a** was obtained using hydroxocobalamin (**1a**:**2a** = 4:1, Table 1, entry 2). No **1a** or **2a** was observed for two other B_{12}-dependent enzymes, methionine synthase and human methylmalonyl-CoA mutase (MetH and hMUT, respectively, Table 1, entries 3 and 4),[6] construction of which is described in the Supporting Information. When reduced to their cob(II)alamin forms using $Na_2S_2O_4$ in the presence of EDA and *p*-methoxystyrene, these enzymes gave trace amounts of cyclopropanation product **3a**,[25] but CarH* showed no detectable cyclopropanation activity (Table S2). Together, these results highlight the unique capability of CarH* to catalyze styrene C−H functionalization.

Table 1. Styrene Alkylation Catalyzed by Hydroxocobalamin and Different B_{12}-Dependent Enzymes

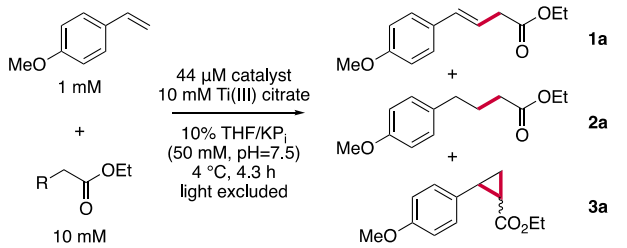

entry	catalyst	1a (%)[a]	2a (%)	3a (%)
1	HOCbl	22(±4)	5(±1)	0
2	CarH*	57(±5)	3(±1)	0
3	MetH	0	0	0
4	*h*MUT	0	0	0

[a]Yields determined by GC/MS analysis of crude reaction mixtures relative to 3,3′,5,5′-tetramethylbenzidine internal standard. Yields and standard deviations for reactions conducted in triplicate are provided. Reactions were conducted in glass vials covered with aluminum foil to exclude light.

Several additional styrenes and diazo substrates were next examined to evaluate the substrate specificity of CarH*-catalyzed styrenyl C−H functionalization (Table 2). CarH* variants containing active-site mutations were also evaluated (Figures S25 and S26), but only the W131F variant provided substantially higher conversions in some cases (Table 2, entries 3 and 6, Figure S26). A modestly good conversion was obtained for electron-rich styrenes, although excellent conversion was observed for an acetamido-substituted styrene (Table 2, entry 4), and the enzyme exhibited a preference for relatively small styrenes and diazoacetates and diazoacetamides. No activity was observed for donor−acceptor or acceptor−acceptor carbene precursors, again highlighting the requirement for relatively small substrates, although phenyl diazoacetate and diethyl diazoacetamide were both tolerated. These results indicate that the protein scaffold plays a role in regulating substrate access to the cobalamin cofactor in CarH* and that the enzyme does not simply serve as a radical initiator as cobalamin does in the absence of the protein scaffold.

Table 2. Substrate Scope of CarH*-Catalyzed Styrene Alkylation

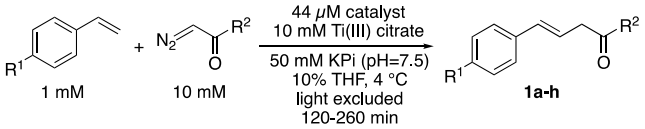

				yield (%)[a]	
entry	1	R^1	R^2	HOCbl	CarH*
1	**a**	OMe	OEt	22(±4)	57(±5)
2	**b**	OEt	OEt	11	22
3	**c**[b]	NMe_2	OEt	20	49
4	**d**	NHAc	OEt	15(±2)	97(±4)
5	**e**	Me	OEt	10	25
6	**f**[b]	H	OEt	8	29
7	**g**	OMe	OPh	13	32
8	**h**	OMe	NEt_2	14	68

[a]Yields determined by GC/MS analysis of crude reaction mixtures relative to 3,3′,5,5′-tetramethylbenzidine internal standard. [b]Reactions were performed using CarH* W131F. Yields and standard deviations for selected reactions conducted in triplicate are provided. Reactions were conducted in glass vials covered with aluminum foil to exclude light.

To gain further insight into the relative reactivity of cob(I)alamin within CarH* versus in solution, the rates for reactions of *p*-methoxystyrene (**1**) and *β,β-d*$_2$-*p*-methoxystyrene (*β,β-d*$_2$-**1**) with EDA in the presence of added CarH* or hydroxocobalamin were next measured in H_2O (Table 3, entries 1 and 3). Due to poor substrate solubility, initial rates (v_i) could only be acquired within a narrow concentration range that prohibited Michaelis−Menten kinetic analysis. Comparing v_i using a 0.5 mM substrate, however, showed that CarH* provides ∼5-fold rate acceleration relative to hydroxocobalamin, consistent with the higher yields obtained from the enzyme under optimized conditions (Table 2). Normal deuterium kinetic isotope effects (KIEs) were observed for styrene alkylation catalyzed by CarH* and hydroxocobalamin (e.g., k_H/k_D = 1.85 and 2.15, respectively, Table 3, entry 1). This finding indicates that C−H cleavage occurs in the rate-limiting step of the reaction, as would be expected if *β*-hydride elimination was at least partially rate-limiting.

The rates for the analogous reactions of **1** and *β,β-d*$_2$-**1** in 50% D_2O/H_2O were also examined to probe the susceptibility of styrene alkylation to solvent isotope effects (SIEs).[26] A normal SIE is observed for hydroxocobalamin ($k_{H_2O}/k_{50\%D_2O}$ >1.4), while an inverse SIE is observed for CarH* ($k_{H_2O}/k_{50\%D_2O}$ < 0.9) (Table 3, entries 1/2 and 3/4). To identify sites in intermediates involved in styrene alkylation that undergo H/D exchange during the reaction and that might therefore play a role in the observed SIEs, gas chromatography/mass spectrometry (GC/MS) was used to analyze products from reactions conducted in 50% D_2O/H_2O. While incorporation of a single deuterium into intermediate **v** was expected based on the mechanism shown in Figure 2A, a mixture of d_1- and d_2-products was obtained. Only slightly higher deuterium incorporation was observed for the CarH*-catalyzed reaction (78% conversion to d_1- and d_2-products vs 66% for hydroxocobalamin), suggesting that this process was not responsible for the observed SIE. No H/D exchange was observed in the reaction of d_8-styrene in H_2O, indicating that

https://doi.org/10.1021/acscatal.1c04748
ACS Catal. 2022, 12, 935−942

Table 3. Deuterium Kinetic Isotope Effects and Solvent Isotope Effects for Styrene Alkylation Reactions Catalyzed by Hydroxocobalamin and CarH*

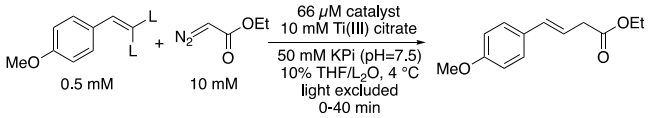

				initial rate (μM·min^{-1})			k_H/k_D		$k_{H_2O}/k_{50\%\ D_2O}$	
entry	styrene	diazo	solvent	CarH*	HOCbl	k_{CarH*}/k_{HOCbl}	CarH*	HOCbl	CarH*	HOCbl
1	**1**	EDA	H_2O	8.87 (0.43)	1.66 (0.08)	5.34 (0.37)	1.85 (0.15)	2.15 (0.15)	0.86 (0.07)	1.67 (0.11)
2	**1**	EDA	50% D_2O/H_2O	10.27 (0.63)	0.99 (0.05)	10.37 (0.82)	1.63 (0.11)	1.86 (0.19)		
3	*β,β-d*$_2$-**1**	EDA	H_2O	4.77 (0.28)	0.77 (0.04)	6.19 (0.50)			0.75 (0.07)	1.45 (0.15)
4	*β,β-d*$_2$-**1**	EDA	50% D_2O/H_2O	6.29 (0.25)	0.53 (0.05)	11.86 (1.86)				

H/D exchange occurs at the *α*-carbon of intermediate **v**, presumably due to acidification by its electrophilic cob(III)alamin center.

Further differences in cob(I)alamin catalysis within CarH* versus in solution were revealed by monitoring methoxystyrene consumption in reactions of **1a** conducted with and without EDA at low conversions (Figure S21). When the CarH*-catalyzed reaction had proceeded to give a 22% yield of **1a**, 24% of the total methoxystyrene had been consumed. In the absence of EDA, however, 43% of styrene was consumed, and polymethoxystyrene oligomers were observed by GPC (Supporting Information Figure S2).[9] During the same period of time, reactions catalyzed by hydroxocobalamin gave only 3% yield of **1a** and 36% of methoxystyrene consumption in the presence of EDA and 52% consumption of methoxystyrene in the absence of EDA.

Finally, we investigated the effects of TEMPO added on CarH* and hydroxocobalamin-catalyzed styrene alkylation.[27] As expected for a reaction involving free-radical intermediates, the yields for the hydroxocobalamin-catalyzed reactions were reduced from 18% to 13% to 7% in the presence of 1 and 5 equiv of TEMPO, respectively (Figure S18). On the other hand, CarH*-catalyzed reactions were not affected by up to 5 equiv of TEMPO. No conversion was observed for either catalyst in the presence of 20 equiv of TEMPO, and the TEMPO adduct of the ethyl carboxymethyl radical was observed by GC/MS analysis of these reaction mixtures (Figure S18).[28] Both d_1- and d_2-TEMPO adducts were obtained for analogous reactions conducted in 50% D_2O/H_2O, consistent with the isotopic exchange at the *α*-carbon noted above.

DISCUSSION

Non-native enzyme catalysis brings the exquisite selectivity of enzymes to bear on chemical reactions that did not happen to emerge in nature. This capability can be revealed by exposing an enzyme to substrates, reagents, or conditions that are distinct from those associated with its native activity but that enable mechanistically feasible pathways involving its active-site residues and cofactors.[29] Particularly illustrative examples of this capability involve the use of heme enzymes as selective catalysts for carbene and nitrene insertion reactions.[30,31] While cytochromes P450 are best known for catalyzing oxene insertions, non-native carbene and nitrene insertion reactions are catalyzed by several heme enzymes with dramatically improved rates and unprecedented selectivity relative to the analogous reactions catalyzed by heme or other iron–porphyrin complexes.

The state of catalysis using vitamin B_{12} derivatives is similar to that employing heme and related complexes. Cobalamins catalyze a broad range of reactions, including reductive olefin coupling, cross-coupling, dehalogenation, and cyclopropanation,[7] but achieving catalyst control over the selectivity of these reactions is challenging since the substituents of the cobalamin corrin ring that could interact with substrates are distal to its cobalt center (Figure 1A). B_{12}-dependent proteins solve this problem by embedding cobalamin cofactors in a chiral protein pocket that regulates substrate access to and reactivity with the cobalt center.[1] As mentioned above, studies on the mechanism of CarH, which involves Co(III)–carbon bond homolysis of its AdoCbl cofactor[18,20] to release 4′,5′-anhydroadenosine (Figure 1B),[16] suggested that it might be uniquely suited for non-native catalysis involving an analogous *β*-hydride elimination (Figure 1C). This hypothesis was validated by successful catalysis of styrene alkylation using EDA in the presence of CarH*.

Several findings from this effort suggest that CarH* and related enzymes could serve as useful starting points for further exploration of non-native cobalamin catalysis. First, the desired activity was observed for CarH but not for the extensively studied B_{12}-dependent enzymes hMUT or MetH.[6] While the poor solubility of CarH initially limited the utility of this finding, this issue was addressed via fusion to MBP to generate CarH*, providing a means to explore the activity of CarH* and perhaps homologous proteins. In addition, observation of the cob(I)alamin form of CarH* using UV–vis spectroelectrochemistry and conversion of this species to others consistent with cob(III)alamin-alkyl complexes upon addition of either EDA or ECA (Figure 2C,D) indicate that this protein can be used to access the non-native Co(I) oxidation state and chemical transformations associated with it.[7]

Most notably, however, the mechanistic studies outlined above indicate that the control exhibited by CarH over the reactivity of the AdoCbl cofactor[16] extends to non-native reactions. The improved styrene alkylation yields and chemoselectivity of cob(I)alamin catalysis within CarH* versus in solution highlight this potential. Improved chemoselectivity is illustrated by both improved production of the desired alkylated styrenes over the corresponding alkane side products under the optimized reaction conditions and, in the presence of added TEMPO, production of alkene over ethyl carboxymethyl–TEMPO adducts. Interestingly, Finke reported that ethylene glycol-induced caging of a [Ado$^{\bullet}$ $^{\bullet}$Cbi] pair uniquely enables *β*-hydride elimination to generate 4′,5′-didehydroadenosine during homolysis of AdoCbi derivatives (Cbi = cobinamide). Ado$^{\bullet}$ could, however, be intercepted

https://doi.org/10.1021/acscatal.1c04748
ACS Catal. 2022, 12, 935–942

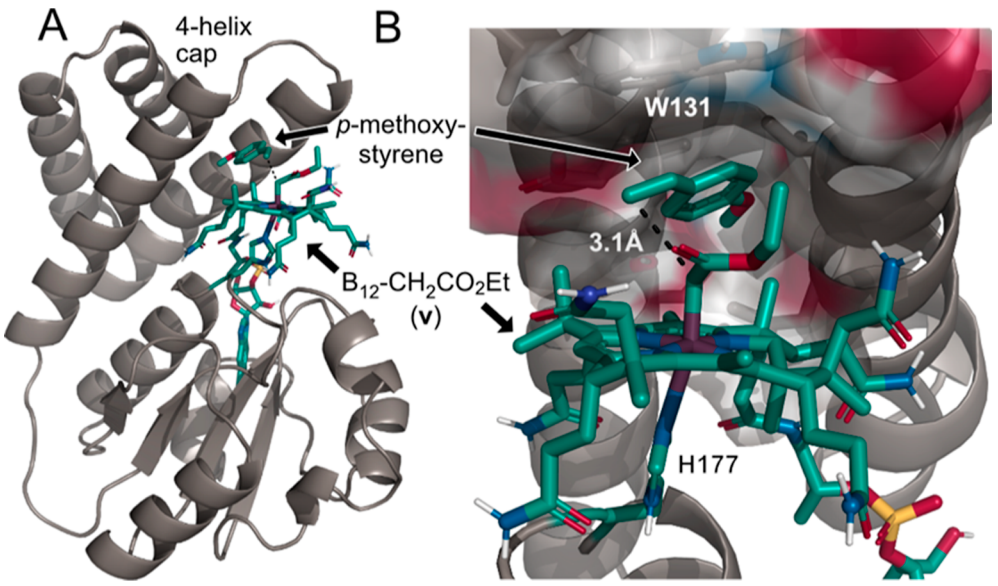

Figure 3. (A) Geometry-optimized structure of ethyl carboxymethyl−Cbl complex **v** (Figure 2A) docked into a structure of CarH (PDB ID: 5C8A).[20] (B) Closeup of active site showing narrow, hydrophobic substrate-binding channel between two helices of the 4-helix cap of CarH (van der Waals surface rendered).

under strong cage conditions using high concentrations of TEMPO to yield an Ado−TEMPO adduct.[27] Drennan suggested that CarH could exert a similar caging effect on Ado$^{\bullet}$ to facilitate β-hydride elimination.[16] The TEMPO trapping studies in the current study suggest that the same phenomenon results in caging of the ethyl carboxymethyl radical that would form upon homolysis of ethyl carboxymethyl−Cbl intermediate **v** (Figure 2A) to enable radical addition to styrene and subsequent β-hydride elimination in preference to cage escape and radical polymerization observed for hydroxocobalamin. Despite this cage effect, high TEMPO concentrations could be used to intercept the α-carboxymethyl radical to generate the corresponding TEMPO adduct of this compound in analogy to the AdoCbl system studied by Finke.[27] While Sension and Penner-Hahn have provided evidence that native CarH activity involves a concerted β-hydride elimination to generate 4′,5′-anhydroadenosine from a triplet metal-to-ligand charge transfer state accessed following photoexcitation,[19] our reactions were conducted in the absence of light, so we presume that this pathway is not operative.

Docking simulations were conducted to show how the CarH* active site might accommodate ethyl carboxymethyl−Cbl intermediate **v** and *p*-methoxystyrene. The dark-state, AdoCbl form of CarH was selected for modeling since its Ado ligand is a better mimic of the non-native ethyl carboxymethyl ligand of **v** than the His132 ligand that binds to Cbl in the light state.[20] Docking a geometry-optimized structure of ethyl carboxymethyl−Cbl (**v**, Figure 2A) into apo-CarH* (Figure 3A) using RosettaLigand shows how the active site might accommodate this alkyl fragment within a narrow binding cleft (Figure 3B). Docking *p*-methoxystyrene into *this* structure shows how sterically undemanding styrenes could access this cleft in an orientation that places the styrene β-position approximately 3 Å from the α-carbon of **v** to enable the observed chemoselectivity. The predicted binding poses (Supporting Information Figure S3) are consistent with the observation that α-substituted diazoacetates are not tolerated but phenyldiazoacetate and *N*,*N*-dimethyldiazoacetamide are tolerated since both project their substituents out of the active site. Likewise, styrene binding within the active site explains why bulky styrene substituents are not tolerated and why the even bulkier TEMPO reacts less readily with **v** to generate the ethyl carboxymethyl adducts that form readily in the presence of hydroxocobalamin. This structure also illustrates how mutation of W131 would be expected to play a role in modulating CarH* reactivity due to its position directly above the putative styrene-binding pocket.

In addition to these reactivity differences, the observed isotope effects also point to the involvement of the CarH* scaffold in modulating cobalamin reactivity. Similar deuterium KIEs are observed for reactions conducted with hydroxocobalamin and CarH*, suggesting that the rate-limiting step of both reactions is the same. The different SIEs and the fact that an inverse SIE is observed for the CarH*-catalyzed reaction in particular suggest that more subtle changes in non-rate-limiting steps may be responsible for the observed selectivity of CarH*.[32] Control reactions conducted in 9% glycerol/H_2O provide similar yields at low substrate conversion to those conducted in pure water (Figure S24), indicating that the increased viscosity of D_2O relative to H_2O is not responsible for the inverse SIE of CarH*.[32] Inverse SIEs for enzyme-catalyzed reactions are most often attributed to displacement of metal-bound waters or H/D exchange involving active-site cysteine residues.[32] CarH does not possess the latter, and cob(I)alamin would not be expected to bind water.[21] Moreover, similar levels of deuterium incorporation into products generated from reactions catalyzed by hydroxocobalamin and CarH* indicate that deuterium exchange involving the substrate is not responsible for the SIE. Inverse SIEs have also been attributed to differences in ligand binding affinity for different conformational states of an enzyme.[33] Given that the four-helix cap that sits on top of the cobalamin cofactor in CarH (Figure 3) is known to undergo large conformational changes,[20] we tentatively suggest that differences in the affinity in those conformation states for cob(III)alamin−alkyl intermediates could explain the observed inverse SIEs and account for the improved selectivity of CarH* relative to cobalamin in solution. Quantitative kinetic analysis and proton

https://doi.org/10.1021/acscatal.1c04748
ACS Catal. 2022, 12, 935−942

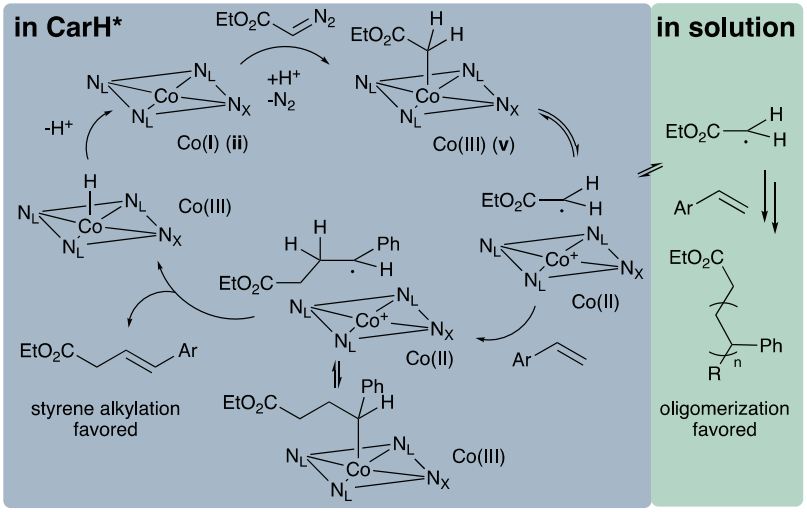

Figure 4. Mechanism of styrene alkylation (adapted from ref 10) accounting for differences in selectivity between cob(I)alamin in CarH* and in solution.

inventory experiments with a suitable model system will be required to better clarify these possibilities.[32,33]

Putting these findings together with the original mechanistic hypothesis of Gryko,[10] we propose that CarH*-catalyzed styrene alkylation proceeds via the mechanism shown in Figure 4. Catalysis is initiated by reduction of aquocobalamin to cob(I)alamin (**ii**), which undergoes oxidative addition with EDA to generate intermediate **v**. Addition of styrene to this complex, presumably via homolysis and recombination of organic radical and cob(II)alamin intermediates,[17] would give a second cob(III)alamin−alkyl complex. β-Hydride elimination from this species would form the observed alkene products and hydridocobalamin, which would undergo deprotonation to reform the cob(I)alamin form of CarH*. In the absence of CarH*, homolytic dissociation of **v** to generate cob(II)alamin and the ethyl carboxymethyl radical can occur. While this species could add back to cob(II)alamin to re-enter the catalytic cycle as suggested by Gryko,[10] polymerization dominates under the reaction conditions used in the current study.

CONCLUSIONS

B_{12}-dependent enzymes are underutilized in biocatalysis relative to other metalloenzymes. Recent examples exploring the substrate scope of native B_{12}-dependent enzyme catalysis[4,34] and the broad range of reactions catalyzed by cobalamin cofactors[7] suggest that suitable systems could find broader application in biocatalysis. This study establishes that a B_{12} protein can catalyze a transformation that diverges substantially from reactivity associated with its native function. While CarH is a transcription regulator that acts via AdoCbl homolysis and β-hydride elimination to generate 4′,5′-didehydroadenosine,[15,16,18,20] CarH* catalyzes styrene C−H alkylation via non-native oxidative addition and olefin addition processes coupled with a native-like β-hydride elimination. Mechanistic studies on this reaction echo findings from earlier studies of AdoCbl homolysis in solution under strong cage conditions and in CarH itself to suggest that CarH* can enable non-native radical chemistry with improved selectivity relative to the cobalamin.[16,27] These findings suggest that engineered CarH* variants and perhaps related B_{12}-dependent enzymes hold great promise as catalysts for a wide range of transformations.

ASSOCIATED CONTENT

Supporting Information

The Supporting Information is available free of charge at https://pubs.acs.org/doi/10.1021/acscatal.1c04748.

Additional experimental details, materials, and methods and $^{1}H/^{13}C$ NMR spectra for all compounds (PDF)

AUTHOR INFORMATION

Corresponding Author

Jared C. Lewis − *Department of Chemistry, Indiana University, Bloomington, Indiana 47405, United States;* orcid.org/0000-0003-2800-8330; Email: jcl3@iu.edu

Authors

Xinhang Yang − *Department of Chemistry, Indiana University, Bloomington, Indiana 47405, United States*

Benjamin H. R. Gerroll − *Department of Chemistry, Indiana University, Bloomington, Indiana 47405, United States*

Yuhua Jiang − *Department of Chemistry, Indiana University, Bloomington, Indiana 47405, United States*

Amardeep Kumar − *Department of Chemistry, Indiana University, Bloomington, Indiana 47405, United States*

Yasmine S. Zubi − *Department of Chemistry, Indiana University, Bloomington, Indiana 47405, United States*

Lane A. Baker − *Department of Chemistry, Indiana University, Bloomington, Indiana 47405, United States;* orcid.org/0000-0001-5127-507X

Complete contact information is available at: https://pubs.acs.org/10.1021/acscatal.1c04748

Notes

The authors declare no competing financial interest.

ACKNOWLEDGMENTS

This study was supported by the U.S. Army Research Laboratory and the U.S. Army Research Office under contract/grant W911NF-19-1-0074 (to J.C.L.), by the NIH (R01 GM115665 to J.C.L.), and by the NSF (CHE-1808133

to L.A.B.). Y.S.Z. gratefully acknowledges receipt of a predoctoral fellowship from the Graduate Training Program in Quantitative and Chemical Biology at Indiana University (T32 GM131994). NMR data were acquired on a spectrometer funded by the NSF (MRI CHE-1920026) using a Prodigy probe that was partially funded by the Indiana Clinical and Translational Sciences Institute. MS data were acquired on a spectrometer funded by NSF grant CHE1726633. We thank Dr. Yi Yi at the Nanoscale Characterization Facility at Indiana University for assistance in preparing and measuring samples for GPC.

REFERENCES

(1) Banerjee, R.; Ragsdale, S. W. The Many Faces of Vitamin B12: Catalysis by Cobalamin-Dependent Enzymes. *Annu. Rev. Biochem.* **2003**, *72*, 209−247.
(2) Marsh, E. N. G.; Drennan, C. L. Adenosylcobalamin-Dependent Isomerases: New Insights into Structure and Mechanism. *Curr. Opin. Chem. Biol.* **2001**, *5*, 499−505.
(3) Ragsdale, S. W. Catalysis of Methyl Group Transfers Involving Tetrahydrofolate and B12. *Vitam. Horm.* **2008**, *79*, 293−324.
(4) Payne, K. A. P.; Quezada, C. P.; Fisher, K.; Dunstan, M. S.; Collins, F. A.; Sjuts, H.; Levy, C.; Hay, S.; Rigby, S. E. J.; Leys, D. Reductive Dehalogenase Structure Suggests a Mechanism for B12-Dependent. *Dehalogenation* **2015**, *517*, 513−516.
(5) Drennan, C. L.; Huang, S.; Drummond, J. T.; Matthews, R. G. How a Protein Binds B12: A 3.0 A X-Ray Structure of B12-Binding Domains of Methionine Synthase. *Science* **1994**, *266*, 1669−1674.
(6) Ludwig, M. L.; Matthews, R. G. Structure-Based Perspectives on B12-Dependent Enzymes. *Annu. Rev. Biochem.* **1997**, *66*, 269−313.
(7) Giedyk, M.; Goliszewska, K.; Gryko, D. Vitamin B12 Catalysed Reactions. *Chem. Soc. Rev.* **2015**, *44*, 3391−3404.
(8) McCauley, K. M.; Pratt, D. A.; Wilson, S. R.; Shey, J.; Burkey, T. J.; Donk, W. A. van der. Properties and Reactivity of Chlorovinylcobalamin and Vinylcobalamin and Their Implications for Vitamin B12-Catalyzed Reductive Dechlorination of Chlorinated Alkenes. *J. Am. Chem. Soc.* **2005**, *127*, 1126−1136.
(9) Shey, J.; McGinley, C. M.; McCauley, K. M.; Dearth, A. S.; Young, B. T.; Donk, W. A. van der. Mechanistic Investigation of a Novel Vitamin B12-Catalyzed Carbon−Carbon Bond Forming Reaction, the Reductive Dimerization of Arylalkenes. *J. Org. Chem.* **2002**, *67*, 837−846.
(10) Giedyk, M.; Goliszewska, K.; Proinsias, K. ó.; Gryko, D. Cobalt(I)-Catalysed CH-Alkylation of Terminal Olefins, and Beyond. *Chem. Commun.* **2016**, *52*, 1389−1392.
(11) Chen, L.; Hisaeda, Y.; Shimakoshi, H. Visible Light-Driven, Room Temperature Heck-Type Reaction of Alkyl Halides with Styrene Derivatives Catalyzed by B12 Complex. *Adv. Synth. Catal.* **2019**, *361*, 2877−2884.
(12) Ikeda, Y.; Nakamura, T.; Yorimitsu, H.; Oshima, K. Cobalt-Catalyzed Heck-Type Reaction of Alkyl Halides with Styrenes. *J. Am. Chem. Soc.* **2002**, *124*, 6514−6515.
(13) Schrauzer, G. N.; Deutsch, E.; Windgassen, R. J. The Nucleophilicity of Vitamin B12s. *J. Am. Chem. Soc.* **1968**, *90*, 2441−2442.
(14) Dolphin, D. Preparation of the Reduced Forms of Vitamin B12 and of Some Analogs of the Vitamin B12 Coenzyme Containing a Cobalt-Carbon Bond. *Methods Enzymol.* **1971**, *18*, 34−52.
(15) Ortiz-Guerrero, J. M.; Polanco, M. C.; Murillo, F. J.; Padmanabhan, S.; Elias-Arnanz, M. Light-Dependent Gene Regulation by a Coenzyme B12-Based Photoreceptor. *Proc. Natl. Acad. Sci. U.S.A.* **2011**, *108*, 7565−7570.
(16) Jost, M.; Simpson, J. H.; Drennan, C. L. The Transcription Factor CarH Safeguards Use of Adenosylcobalamin as a Light Sensor by Altering the Photolysis Products. *Biochemistry* **2015**, *54*, 3231−3234.
(17) Baldwin, D. A.; Betterton, E. A.; Chemaly, S. M.; Pratt, J. M. The Chemistry of Vitamin B 12. Part 25. Mechanism of the β-Elimination of Olefins from Alkylcorrinoids; Evidence for an Initial Homolytic Fission of the Co−C Bond. *J. Chem. Soc., Dalton Trans.* **1985**, *8*, 1613−1618.
(18) Kutta, R. J.; Hardman, S. J. O.; Johannissen, L. O.; Bellina, B.; Messiha, H. L.; Ortiz-Guerrero, J. M.; Elías-Arnanz, M.; Padmanabhan, S.; Barran, P.; Scrutton, N. S.; Jones, A. R. The Photochemical Mechanism of a B12-Dependent Photoreceptor Protein. *Nat. Commun.* **2019**, *6*, 1−11.
(19) Miller, N. A.; Kaneshiro, A. K.; Konar, A.; Alonso-Mori, R.; Britz, A.; Deb, A.; Glownia, J. M.; Koralek, J. D.; Mallik, L.; Meadows, J. H.; Michocki, L. B.; van Driel, T. B.; Koutmos, M.; Padmanabhan, S.; Elías-Arnanz, M.; Kubarych, K. J.; Marsh, E. N. G.; Penner-Hahn, J. E.; Sension, R. J. The Photoactive Excited State of the B12-Based Photoreceptor CarH. *J. Phys. Chem. B* **2020**, *124*, 10732−10738.
(20) Jost, M.; Fernández-Zapata, J.; Polanco, M. C.; Ortiz-Guerrero, J. M.; Chen, P. Y.-T.; Kang, G.; Padmanabhan, S.; Elías-Arnanz, M.; Drennan, C. L. Structural Basis for Gene Regulation by a B12-Dependent Photoreceptor. *Nature* **2015**, *526*, 536−541.
(21) Lexa, D.; Savéant, J. The Electrochemistry of Vitamin B12. *Acc. Chem. Res.* **1983**, *16*, 235−243.
(22) Lexa, D.; Savéant, J. M.; Zickler, J. Electrochemistry of Vitamin B12. 2. Redox and Acid-Base Equilibria in the B12a/B12r System. *J. Am. Chem. Soc.* **1977**, *99*, 2786−2790.
(23) Hill, J. A.; Pratt, J. M.; Williams, R. J. P. The Chemistry of Vitamin B 12 . Part I. The Valency and Spectrum of the Coenzyme. *J. Chem. Soc.* **1964**, *0*, 5149−5153.
(24) Lexa, D.; Savéant, J.-M. Brönsted Basicity of Vitamin B12s. *J. Chem. Soc., Chem. Commun.* **1975**, *21*, 872−874.
(25) Chen, Y.; Zhang, X. P. Vitamin B 12Derivatives as Natural Asymmetric Catalysts: Enantioselective Cyclopropanation of Alkenes. *J. Org. Chem.* **2004**, *69*, 2431−2435.
(26) Quinn, D. M.; Sutton, L. D. Enzyme Mechanism from Isotope Effects. In *Theoretical Basis and Mechanistic Utility of Solvent Isotope Effects*; Cook, P. F., Ed., 1991, pp 73−126.
(27) Garr, C. D.; Finke, R. G. Radical Cage Effects in Adocobinamide (Axial-Base-Off Coenzyme B12): A Simple Method for Trapping [Ado• •CoII] Radical Pairs, A New Beta-H Elimination Product from the Radical Pair, and Measurement of an Unprecedentedly Large Cage-Recombination Efficiency Factor, Fc>0.94. *J. Am. Chem. Soc.* **1992**, *114*, 10440−10445.
(28) Finke, R. G.; Hay, B. P. Thermolysis of Adenosylcobalamin: A Product, Kinetic, and Cobalt-Carbon (C5') Bond Dissociation Energy Study. *Inorg. Chem.* **1984**, *23*, 3041−3043.
(29) Khersonsky, O.; Tawfik, D. S. Enzyme Promiscuity: A Mechanistic and Evolutionary Perspective. *Annu. Rev. Biochem.* **2010**, *79*, 471−505.
(30) Yang, Y.; Arnold, F. H. Navigating the Unnatural Reaction Space: Directed Evolution of Heme Proteins for Selective Carbene and Nitrene Transfer. *Acc. Chem. Res.* **2021**, *54*, 1209−1225.
(31) Brandenberg, O. F.; Fasan, R.; Arnold, F. H. Exploiting and Engineering Hemoproteins for Abiological Carbene and Nitrene Transfer Reactions. *Curr. Opin. Biotechnol.* **2017**, *47*, 102−111.
(32) Fernandez, P. L.; Murkin, A. S. Inverse Solvent Isotope Effects in Enzyme-Catalyzed Reactions. *Molecules* **2020**, *25*, 1933.
(33) Pollard-Knight, D.; Cornish-Bowden, A. Solvent Isotope Effects on the Glucokinase Reaction. *Eur. J. Biochem.* **1984**, *141*, 157−163.
(34) Grimm, C.; Lazzarotto, M.; Pompei, S.; Schichler, J.; Richter, N.; Farnberger, J. E.; Fuchs, M.; Kroutil, W. Oxygen-Free Regioselective Biocatalytic Demethylation of Methyl-Phenyl Ethers via Methyltransfer Employing Veratrol-O-demethylase. *ACS Catal.* **2020**, *10*, 10375−10380.

https://doi.org/10.1021/acscatal.1c04748
ACS Catal. 2022, 12, 935−942